RESEARCH ARTICLE

Neighbours matter and the weak succumb: Ash dieback infection is more severe in ash trees with fewer conspecific neighbours and lower prior growth rate

David J. Cracknell[1] | George F. Peterken[2] | Arne Pommerening[3] |
Peter J. Lawrence[4] | John R. Healey[1]

[1]School of Natural Sciences, Bangor University, Bangor, UK

[2]Beechwood House, Lydney, UK

[3]Department of Forest Ecology and Management, Swedish University of Agricultural Sciences, Umeå, Sweden

[4]Institute of Science and Environment, University of Cumbria, Ambleside, UK

Correspondence
David J. Cracknell
Email: cracknelldavid@gmail.com

Handling Editor: Anne Kempel

Abstract

1. The epidemiology and severity of ash dieback (ADB), the disease caused by the ascomycete fungus *Hymenoscyphus fraxineus*, has been linked to a variety of site conditions; however, there has been a lack of analysis at an individual tree scale.

2. Symptoms of ADB were scored on ca. 400 trees of *Fraxinus excelsior* (ash) in permanent sample plots during two successive years in a UK natural woodland reserve. Using comprehensive plot records maintained since 1945, and detailed spatial records updated since 1977, we assembled an array of potential explanatory variables, including site environment factors, ash tree density, previous and present tree condition and near neighbourhood summary statistics (NNSS), such as species mingling and size dominance. Their impact on the severity of ADB of focal ash trees was tested with generalised linear mixed effects models (GLMM).

3. The severity of ADB was much greater in the lower slope parts of the site with moister soils and least in a managed area subject to tree thinning in the previous 35 years. Severity of ADB had a negative association with focal ash tree prior relative growth rate over a period of a decade immediately before the disease was detected at the site. Greater ADB severity was also significantly associated with smaller diameter at breast height of ash trees. Additionally, ADB was significantly positively associated with a greater proportion of heterospecific trees amongst the six nearest neighbours of the focal tree.

4. *Synthesis*. The relationship of the severity of ADB disease with site environment, tree condition and neighbourhood is complex but nevertheless important in the progression of the disease. The findings suggest some silvicultural interventions, such as thinning to increase the vigour of retained ash trees, might reduce the impact of ADB.

KEYWORDS
basal area of larger trees, chalara, forest dynamics, size dominance, species mingling, tree diameter, tree disease, tree pathogen

1 | INTRODUCTION

Ash dieback (ADB) disease, caused by the ascomycete fungus *Hymenoscyphus fraxineus*, has plagued European woodlands for nearly three decades. It has spread rapidly from East to West across the continent causing a major impact on ash populations and large areas of ash-dominated woodlands. In Europe, ADB was first recognised in Poland in the early 1990s (Kowalski, 2006) and was positively identified as arriving in Great Britain by 2012, since when it has infected populations of European ash (*Fraxinus excelsior*) across most of the UK (British Ecological Society, 2012; Pautasso et al., 2013; Stocks et al., 2017). There have been many location- and country-specific reports of ADB-linked ash mortality from across Europe. However, predicting eventual mortality rates in mature ash trees is difficult due to the slow progression of the disease. Therefore, Coker et al. (2019) carried out a meta-analysis of published studies, together with a time-dependent model, to estimate longer-term mortality, leading to a pan-European prediction (with wide confidence intervals) of approximately 60% average cumulative mortality in natural woodland. However, plantation trials of young trees have shown that only 1%–5% of the populations are genetically tolerant of ADB (e.g. Kjær et al., 2012; Stocks et al., 2017). Nevertheless, it is likely that ADB will have a lasting impact on the 953 animal and plant species associated with *F. excelsior* (Mitchell et al., 2014). ADB is one of the most researched topics in recent European woodland ecological literature, yet half of the studies involved laboratory-based experiments rather than in situ observations (Bowler, 2019). At present, there is no effective silvicultural or other management response to slow the spread of the disease, once it has arrived in a region (Skovsgaard et al., 2017). Therefore, the primary focus has been on the long-term strategy of tree selection and breeding for resistance as the basis for restoration of ash populations (McKinney et al., 2014).

The disease induces symptoms of leaf wilting, dieback of twigs in the crown, and necrotic lesions in young shoots, bark, and leaf petioles. The clearest visible symptoms are epicormic sprouting on the trunk and branches (Enderle et al., 2018). Ascospores develop in the apothecia of leaf rachises after they fall during the autumn and winter, and the following spring and summer they are released and dispersed by wind (Gross et al., 2014; Timmermann et al., 2011, 2017), leading to new infections and continuation of the cycle (Nemesio-Gorriz et al., 2019). This suggests that proximity to an infected tree will influence the probability and severity of infection. Inoculum density decreases rapidly up to 50 m from infected trees (Chandelier et al., 2014; Grosdidier et al., 2018); however, it is estimated that the mean dispersal distance of ascospores is between 0.2 and 2.6 km, depending on the scale and dispersal kernel (statistical distribution of distances) fitted (Grosdidier et al., 2018).

The level of disease in the population of ash within a woodland is positively associated with various site factors, including air humidity and temperature, topography, occurrence and dimensions of watercourses, soil type and moisture (Chumanová et al., 2019; Erfmeier et al., 2019; Grosdidier et al., 2020; Havrdová et al., 2017; Klesse et al., 2021; Skovsgaard et al., 2017). Woodland structural and compositional factors may

have an influence on ADB, including local tree density, light levels and tree species mixtures (Chumanová et al., 2019; Erfmeier et al., 2019). Furthermore, research has suggested that individual tree metrics may be correlated with ADB. Larger diameter trees, for example, have been found to display milder symptoms with a slower progression of ADB in the crown (Enderle et al., 2019; Havrdová et al., 2017; Lenz et al., 2016; Marçais et al., 2016; Queloz, 2016; Skovsgaard et al., 2010). Previous studies also indicate that smaller and slower-growing trees are more susceptible to ADB and have higher mortality rates than larger, faster-growing individuals (Enderle et al., 2018, 2019; Klesse et al., 2020, 2021; Marçais et al., 2017).

Recent research on the landscape epidemiology of ADB in northern France concluded that *F. excelsior* trees in isolated agricultural settings were less affected by the disease than those within forests (Grosdidier et al., 2020). This can be attributed to differences in microclimate, with higher crown temperatures in isolated trees that may restrict pathogen development, and/or to lower host density (as found in a grassland biodiversity experiment by Mitchell et al., 2002). A previous large-scale study of ash forests in the Czech Republic also suggested that higher tree density and the proximity of certain tree species (such as *Quercus robur* and *Fagus sylvatica*), together with proximity to the nearest ash stand, as well as physical site environmental factors, can worsen the impact of the disease (Havrdová et al., 2016, 2017). Similarly, a nationwide study in Switzerland found higher mortality probability in stands with humid microclimate and high abundance of ash (Klesse et al., 2021). Thus, as well as the severity of ADB being linked to forest microclimate, proximity and density of infected ash hosts has a major influence on the rate of spore arrival on a susceptible tree.

The present study sought to determine the impact of a range of site environment, previous and present tree condition and near neighbourhood factors on the severity of ADB in a population of *F. excelsior* trees. The specific questions were: (1) Is the severity of ADB greater with increasing tree density in the immediate neighbourhood of the focal tree? (2) Is the severity of ADB less in trees that had a greater prior growth rate? (3) Is the severity of ADB less in trees that had a greater crown dominance over their immediate neighbourhood? (4) Is the severity of ADB less in trees whose neighbourhood is more dominated by heterospecific trees?

To answer these questions, we carried out a study during the early-mid stages of a developing ADB epidemic at Lady Park Wood, Monmouthshire, Wales, which has a well-established ash population in near natural growing conditions—most of the woodland has been left unmanaged for more than 70 years—as well as records of individual trees in permanent sample plots since 1945.

2 | MATERIALS AND METHODS

2.1 | Study site

The study site, Lady Park Wood, is a 36-hectare ancient woodland nature reserve containing 33 native tree and shrub species, dominated by *Tilia platyphyllos*, *Tilia cordata*, *Fagus sylvatica*, *Fraxinus*

excelsior, *Betula* spp., *Quercus petraea*, *Ulmus glabra* and *Taxus baccata*. The soil across the woodland is heterogeneous; its span of pH is one of the widest ranges in a single British woodland—from 7.9 to 3.8 (Peterken & Mountford, 2017) despite limestone being the dominant bedrock. Soil pH was measured in 288 samples over 72 evenly distributed 200 m² plots (Peterken & Mountford, 2017), which we subsequently mapped onto the tree sample subplots described below. GPS altitude readings were taken in each subplot and used to calculate its mean slope gradient angle.

The long history of monitoring at the site provides rare longitudinal records from repeated censuses of all trees in 10 long thin permanent sample plots, termed 'transects'. All are 19.8 m wide and oriented parallel with the slope, but they vary in length from 150 to 500 m (Figure 1). The transects have historically been categorised and subdivided depending on when there was last human-caused disturbance, for example coppicing or thinning, and also by topographic position or dominant soil type. In Figure 1 and Table 1, we have sought to clarify the classification of these zones within the site, which define the nonoverlapping 'stand types' analysed in this study.

Nine of the transects (I–IX) are in woodland unmanaged for 78 years, which has been enclosed by a two-metre-high deer fence since 2007. There is considerable variation amongst and within them in both topographic position and past management. Above the limestone cliff that bisects the woodland into upper and lower sections, transects I–V each sample both 'old growth' and 'young growth' stands (Figure 1). The former was last coppiced in 1870 and the latter in 1942 just before the site became a reserve. Transect VI predominantly samples 'young growth' woodland on well-drained soils of what is known as the 'colluvial fan'. Transects VII-IX are shorter being confined to the woodland below the limestone cliff. These 'below cliff' stands are ecologically distinct being on steeply sloping ground and affected by some felling of *Tilia* spp. in 1942 for aircraft production; they have a higher relative density of *F. excelsior* and *Ulmus glabra* than in the other stands. Transect X was added in 1984 in an adjacent 'managed' unfenced compartment, the majority of which has been thinned twice since then. Metrics of each stand type are given in Table 4.

Hand-drawn maps of the locations of the centre of each individual woody plant ≥1.3 m height in transects I–VI were recorded on a Cartesian coordinate grid by reference to transect edge markers with a regular 30.5-m spacing in 1977. Transects VII–X were similarly mapped in 1984–85. These records were updated and checked for accuracy at each successive enumeration of each transect, including in 2013 before ADB was first observed in the woodland and in anticipation of its arrival. For the present study, these maps were scanned digitally using Esri ArcGIS Pro® 2.7.3 (2021) software onto Ordnance Survey digital maps and allocated their British National Grid coordinate values. The geographical location of the centre of each tree was normalised for slope. After the initial enumeration of each transect, all woody plants ≥1.3 m height (with no minimum diameter limit) in transects I–IX were identified to species, recorded as live or dead and measured for diameter at breast height (1.3 m,

dbh) in 1955, 1977 and 1983 and in all 10 transects in 1986, 1992, 2000, 2002, 2010, 2013 and 2018. In the case of the many multiple-stemmed coppice stools, an equivalent single diameter was assigned, calculated from the sum of their stem cross-sectional areas.

2.2 | Tree attributes

A total of 464 *F. excelsior* trees across the 10 permanent transects, representing all live individuals ≥1.3 m height at the start of the study in 2019, were assessed for ADB symptoms in July and August 2019 and 381 during August 2020. The lower number in the second year is due to the increased constraint on fieldwork due to risk assessment and restriction of available time under that constraint. Therefore, our main statistical models were only applied to the more complete data set recorded in 2019. We have used the 2020 data solely to assess the overall rate of progression of the disease at the time of the study. The data collection was undertaken under licence from Natural England National Nature Reserve Permit LPW/07-19/02, which allowed observers access to the site from 15 July 2019 to 30 September 2020.

The severity of crown dieback was scored between 0 and 100% based on a visual estimation of proportionate level of defoliation, similar to the assessment methods used in other studies of ADB (Grosdidier et al., 2020; Lenz et al., 2012; Turczanski et al., 2020). Two observers surveyed each focal tree according to an agreed scale of crown defoliation in scoring classes of 0%–10%, 10%–20%, 20%–30%, 30%–40%, 40%–50%, 50%–60%, 60%–70%, 70%–80%, 80%–90% and 90%–100%, with their assessments calibrated at regular intervals against photographs of previously agreed percentage defoliation scores to ensure scoring did not drift over the study. Independent scoring of the same tree by each of the observers was conducted periodically to guard against observer bias and the scoring of the transects was carried out in random order to avoid confounding with topographic/stand type. Ash trees with a score of 0% crown dieback and no trunk sprouting or other visible sign of infection were classified as uninfected.

Annual mortality rate (AMR) of ash, as a simple indicator of change from before to after the onset of ADB in the study woodland, was calculated using the formula of Sheil et al. (1995): $AMR = 1 - (N_1/N_0)^{1/t}$, where N is the number of trees alive at each census and t is the number of years between census 0 and census 1. Two periods of recorded prior growth rates were selected: 1977 to 2013, and 2000–2002 to 2013. Basal area of each tree was also calculated from the dbh measurements as an explanatory variable in its own right for focal ash trees, but also to calculate further explanatory variables, such as the total basal area of the stand. Basal area of larger trees (bal), an indicator of the level of competition for light on the focal tree at the stand level (Pommerening & Grabarnik, 2019; Wykoff, 1990), was calculated as the total basal area of all trees larger than or equal to the basal area of the focal tree i in the same subplot at a particular time t (Table 2, Formula 5). By 'sub-plot', here we mean the regular subdivisions of the transect plots permanently
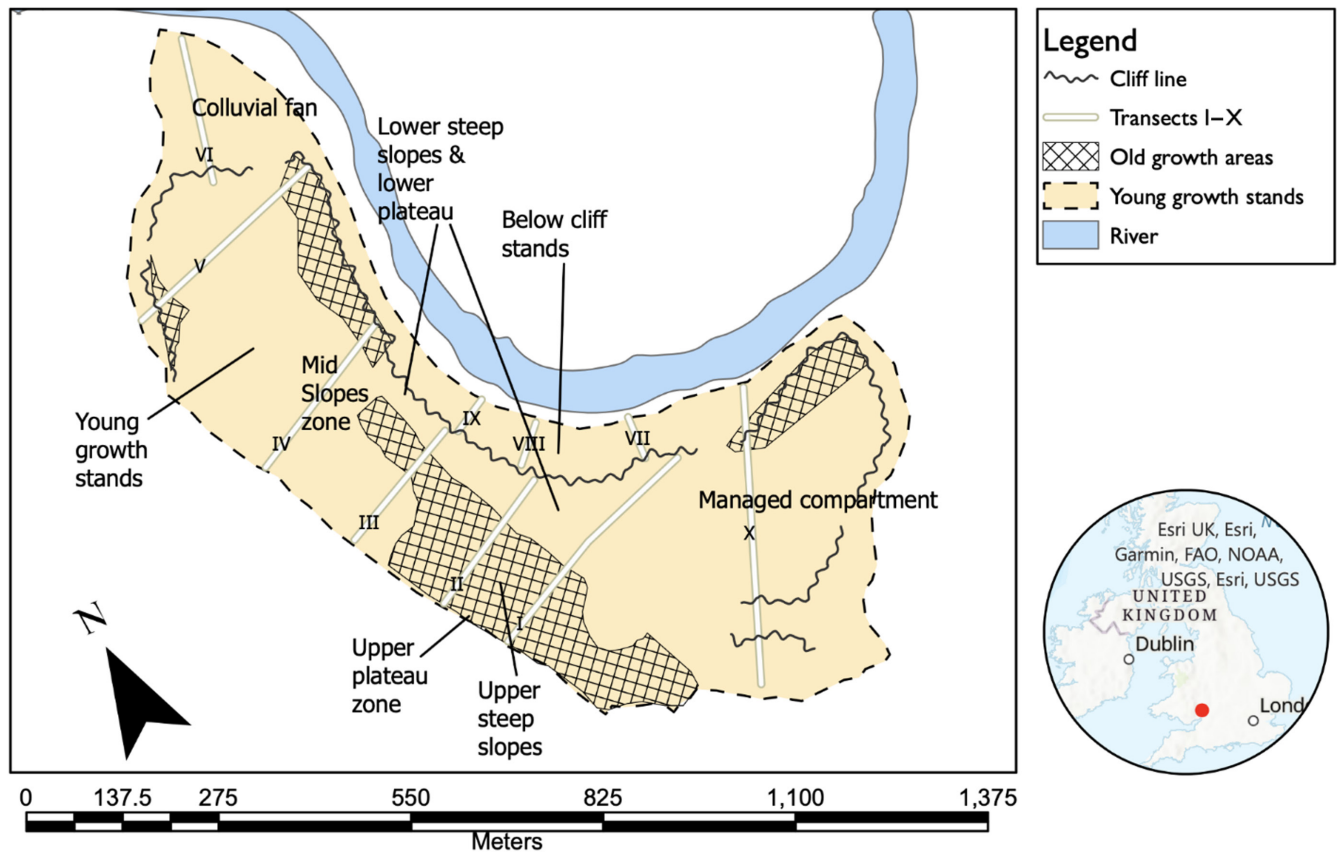
FIGURE 1 Map of Lady Park Wood, Monmouthshire, Wales, with the geographical location shown in the inset map. Stands in the unshaded areas ('young growth') were felled in 1942–3, leaving a shelterwood of larger individuals; the shaded areas ('old growth') were last coppiced ca. 150 years ago. Transects VII, VIII and IX occupy a separate topographic position with outcropping limestone and steep slopes: the 'below cliff' stand, which is ecologically distinctive as the ground is much steeper, some felling took place in the early 1940s, and the relative density of *Fraxinus excelsior* and *Ulmus glabra* is higher than in the other stands. Transects I–VI were laid out and first recorded in 1944, VII–IX in 1955 and X in 1984. The majority of transect X is in stands thinned in 1984 and 1994, the 'managed compartment', but there is some old growth at the cliff end and a small section of young growth at the top of the slope. The 'colluvial fan' in the northern section of the wood is sampled by the lower two-thirds of Transect VI. Also shown are topographical zones, which differ in soil type and slope gradient, such as 'mid slopes', 'lower steep slopes' and 'upper plateau'.

marked by stakes at 400-ft (121.9-m) intervals down the slope, which were used for ease and accuracy of the successive enumerations of the transects but were also, it transpired during our study, the most ecologically appropriate for near-neighbour spatial analysis. The size of each subplot of the transects was 19.8 m × 121.9 m (2414 m²), and they were arranged so that each lay entirely within either the 'old growth' or 'young growth' stands. An alternative measure of a focal tree's crown dominance relative to its neighbours was provided by the recording, in previous enumerations, of each tree's crown position in four categories: ground, understorey, subcanopy and canopy.

2.3 | Spatial analysis

Spatial point process methods were used to compute the Euclidean distances between nearest neighbour points within each 2414 m² subplot (as illustrated in Figure 2). The 'spatstat' package in R was used to estimate near neighbour summary statistics (NNSS). Using 'spatstat', a number of established individual tree neighbourhood

indices were calculated (Baddeley et al., 2015; Illian et al., 2008; Pommerening & Grabarnik, 2019) for use as explanatory variables, as outlined below. We used the minus-sampling 'NN1' nearest neighbour edge-correction method outlined by Pommerening and Grabarnik (2019), in turn based on Hanisch (1984), for all these NNSS.

2.3.1 | Species mingling (mi) and weighted species mingling (wmi)

Both species mingling (mi) and richness-weighted species mingling (wmi) are spatially explicit diversity indices. Species mingling (mi) is a calculated value between zero and one representing the proportion of heterospecific (rather than conspecific) trees in the near neighbourhood of the focal tree (Table 2, Formula 1). So, if there are four neighbours counted and three are heterospecific, the focal tree is given a species mingling value of 0.75. The total number of nearest neighbours (k) can be varied according to the ecological context. We used a version of the formula which incorporates weighting by the number of

TABLE 1 Distribution of the number of 30.5-m (100-ft) length transect sections amongst topographic and management history stand types in each of the 10 transects.

Transect	Old growth (OG)	Young growth (YG)	Colluvial fan (CF)	Below cliff (BC)	Managed compartment (MC)	Total number
I	5	5	–	–	–	10
II	5	2	–	–	–	7
III	2	5	–	–	–	7
IV	3	7	–	–	–	10
V	4	7	–	–	–	11
VI	–	2	4	–	–	6
VII	–	–	–	3	–	3
VIII	–	–	–	4	–	4
IX	–	–	–	3	–	3
X	2	–	–	1	12	15
Total number	21	28	4	11	12	76
Total area (m^2)	12,680	16,910	2420	6640	7250	45,900

*Note*: Each section has an area of 604 m^2. There is no overlap between the stand types.

TABLE 2 Key formulae used to calculate the indices. k in all equations relates to the total number of nearest neighbour trees considered in the formulae.

Equation	Variable name	Variable category	Formula	NNSS definition
Near neighbourhood summary statistics (NNSS) formulae				
(1)	Species mingling (Gadow, 1993)	Species	$M_i = \frac{1}{k} \sum_{j=1}^{k} \mathbf{1}(species_i \neq species_j)$	$M_i \in [0,1]$
(2)	Weighted species mingling (Hui et al., 2011; Wang et al., 2021)	Species	$M_i' = \frac{1}{k \cdot c} \sum_{j=1}^{k} \mathbf{1}(species_i \neq species_j) \cdot s_i$	s_i is species richness amongst k nearest neighbours of an including tree i; $c = \min(S, k+1)$, where S is total species richness of forest stand
(3)	Size dominance (Aguirre et al., 2003; Hui et al., 1998)	Size	$U_i = \frac{1}{k} \sum_{j=1}^{k} \mathbf{1}(m_i > m_j)$	$U_i \in [0,1]$
(4)	Local density (Baddeley et al., 2015; Diggle, 1985)	Density	$\hat{\lambda}_t(x) = \left\{ \sum_{i=1}^{n} \delta_t(x - x_i) \right\} / p_t(x)$	$\hat{\lambda}_t$ = local intensity of focal trees x_i, $\delta(x)$ = kernel function, and $p_t(x)$ = end correction
Focal tree attributes formulae				
(5)	Basal area of trees > focal tree (Pommerening & Grabarnik, 2019; Wykoff, 1990)	Size	$BAL_i(t) = G(t) \cdot (1 - p_i(t))$ with $p_i(t) = \frac{1}{G(t)} \sum_{\leq g_i(t)} g_i(t)$	Where i is a given tree at time t, basal area percentile is $p_i(t)$ of tree i denoting relative dominance, where $G(t)$ is basal area ha^{-1} of forest stand at time t.
(6)	Basal area of tree (Gadow et al., 2021)	Size	$BA = \frac{\pi}{4} \cdot \sum_{i=1}^{n} dbh_i^2$ in cm^2 $BA = \frac{\pi}{40000} \cdot \sum_{i=1}^{n} dbh_i^2$ in m^2	dbh is diameter at breast height or 1.3 m.
Stand attributes formulae				
(7)	Basal area of forest stand (Pommerening & Grabarnik, 2019)	Size	$G = \frac{\sum_{i=1}^{n} g_i}{A}$	g_i is basal area of tree i in m^2, N is number of trees in stand, A is area of sample plot in ha

species in the k nearest neighbours, known as 'richness-weighted species mingling' (wmi; Hui et al., 2011), with the weighting effect limited by the number of species present in the focal tree's subplot (which sets the maximum possible number of species in $k+1$ trees at that location;

Wang et al., 2021; Table 2, Formula 2). The wmi index is thus a more sophisticated version of the mingling index, which encompasses the component of species richness in a tree's heterospecific near neighbourhood, producing a greater variation in index values between

FIGURE 2 Locations and species of all trees in two transect subplots (19.8 m × 121.9 m) generated using the 'spatstat' R package showing the prevalence of ADB. (a) is an example of one of the 'old growth' subplots in transect 1. (b) is one of the 'young growth' subplots in transect 3. The red dots are infected *Fraxinus excelsior* trees, with their size representing the severity of infection. Asymptomatic *F. excelsior* trees are shown as open circles. The data illustrated in these spatial plots were used to calculate species mingling, size dominance and tree density.
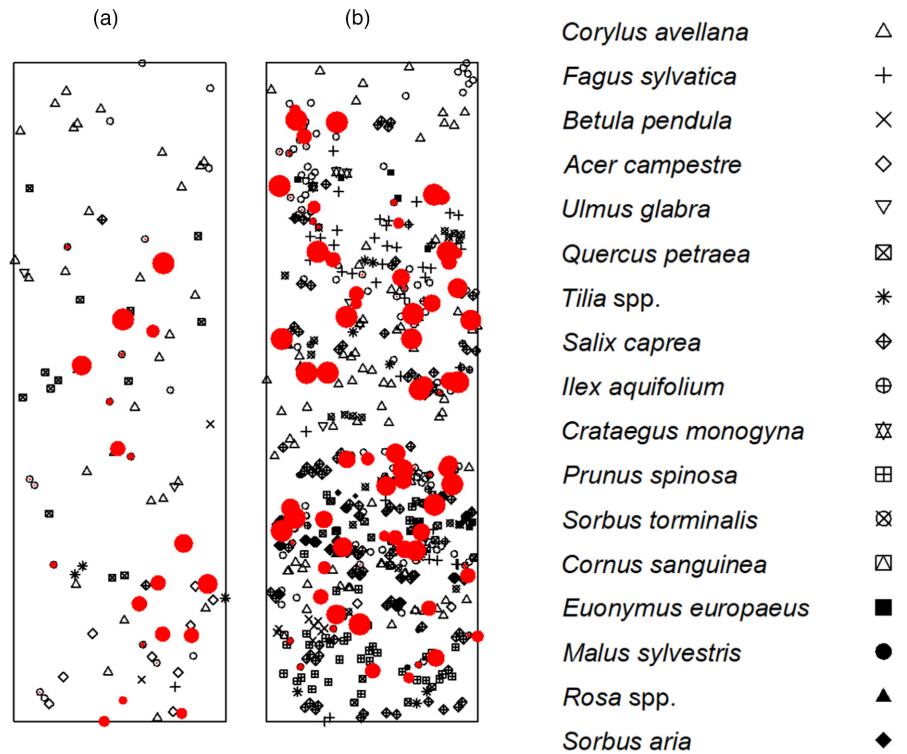
trees. However, to test the use of wmi for assessing the dominance of ash trees' neighbourhoods by heterospecific trees, we examined the linear correlation of wmi with mi for the 464 ash trees included in the study; the Pearson correlation coefficient (*r*) was 0.89 giving us full confidence in selecting wmi for this purpose.

2.3.2 | Size dominance (ui)

The size dominance index (ui) measures the size of a focal tree relative to its *k* nearest neighbours (Table 2, Formula 3). We used stem diameter (dbh) to describe size, but other size characteristics are also possible. The calculation of this index is similar to that of the species mingling index, with a value between zero and one, and the potential to vary *k* (Aguirre et al., 2003; Hui et al., 1998; Pommerening & Grabarnik, 2019).

2.3.3 | Local tree density (λ)

Local tree density around a focal tree (λ) was calculated using a kernel smoothing function in R (Baddeley et al., 2015). It was originated by Diggle (1985) as 'a method for estimating the local intensity' as a point process, and it includes edge correction within the formula (Table 2, Formula 4).

2.4 | Statistical analysis

The complex dataset of Lady Park Wood is derived from a range of historical and primary sources, as described above, which do not always overlap precisely and as such cannot be coerced into a single overarching statistical model. We have therefore categorised the potential predictor variables into two groups, which we have termed as 'non-spatial', dominated by edaphic and context-related variables, and by spatially explicit point process statistical characteristics (Table 3). Variables that exist in both categories did not require postprocessing in that they remain true to their original sources and coincidentally provide a useful bridge between the two groups. The historical sampling strategy was based on dividing the site into several different stand types and topographical zones. Our statistical methods were selected, knowing that the sampling and methods had all the hallmarks of being nested and hierarchical (Wang et al., 2019). We used a model averaging approach (Dormann et al., 2018).

Prior to the modelling, we investigated the most plausible distribution of our response variable (adb19) using the 'fitdistrplus' package, identifying a beta distribution as the most appropriate family for the models (Supporting Information; Delignette-Muller et al., 2015; Zuur et al., 2009). For selection of the predictor variables to include in the models, we assessed likelihood of collinearity amongst our full set of variables using Pearson's correlation. Where variable pairs were strongly correlated (>0.7), only one variable was retained. We then identified variables that could not logically co-occur as predictors (due to legacy methods and/or variables being derivatives of each other). An example of inappropriate or at the very least uninterpretable inference might result from modelling of species mingling at more than one of 4, 5 and 6 nearest neighbour tree ranges. Where pairs could not be precluded due to collinearity, a selection criterion for one of these pairs was applied using the lowest Akaike information criterion (adjusted for small sample size AICc) using the

TABLE 3 List of response and predictor variables obtained from Lady Park Wood showing their potential for inclusion in nonspatial and spatial models.

	Description	Nonspatial model	Spatial model
Epidemiological (response) variable			
adb19	Disease score in 2019 (% converted to 0–1 scale for beta distribution)	●	●
Site/edaphic/focal tree attribute predictors			
stand type	Old growth (OG), young growth (YG), below cliff (BC), colluvial fan (CF), managed compartment (MC) with thinned subcompartments MC1 and MC2	●	●
transect	Transect number	●	●
pH	Soil pH	●	
gradient	Slope gradient (degrees)	●	
ash density	Density of *Fraxinus excelsior* trees in the subplot	●	
dbh77	Focal tree 1977 diameter at breast height (cm)	●	
dbh02	Focal tree 2000–2 diameter at breast height (cm)	●	
dbh13	Focal tree 2013 diameter at breast height (cm)	●	●
can19	Focal tree canopy score in 2019	●	
rgr-l	Focal tree log relative growth rate—long time period (1977 to 2013)	●	
rgr-s	Focal tree log relative growth rate—short time period (2000–2002 to 2013)	●	
Point process statistics predictors			
wmi4	Weighted species mingling ($k=4$)		●
wmi5	Weighted species mingling ($k=5$)		●
wmi6	Weighted species mingling ($k=6$)		●
ui4	Size dominance ($k=4$)		●
ui5	Size dominance ($k=5$)		●
ui6	Size dominance ($k=6$)		●
ba	Basal area		●
bal	Basal area of larger trees in subplot		●
lambda	Local tree density		●

Note: Log relative growth rate—short time period (rgr-s) data are not available for the managed compartment only due to lack of site access during 2000–2002. Formal definitions of the point process statistics are provided in Table 2.

'AICcmodavg' package (Mazerolle & Mazerolle, 2017). This process reduced the possible predictor variables in the nonspatial set to seven, with 128 model permutations, and in the spatial set to six variables, with 64 model permutations.

For the model averaging stage of our procedure, we started with an initial 'global model' for each of the nonspatial and spatial models (formulae shown in Supporting Information). We used sampling 'transect' number (1–10) as a random effect and visually checked residuals for performance and comparison against the null model (Zuur et al., 2009). From the 128 nonspatial and 64 spatial model permutations, we retained what are often defined as the 'top models' for each using the 'MuMIn' package

(Bartoń, 2022) based on delta AICc <2, as scores between 0 and 2 can be broadly considered equivalent despite potentially different combinations of predictors (Burnham et al., 2011; Wagenmakers & Farrell, 2004). All seven predictor variables were present in the nonspatial top models, but one (ui6) was absent from the spatial top models (retaining the other five). These sets were then averaged and explored. To assess the effect of selecting the weighted mingling index (wmi) rather than the basic species mingling index (mi) a sensitivity analysis was carried out of the effect on the top models of switching from wmi to mi. All the statistical analyses were conducted in the R programming language and R Studio (R Core Team, 2021). A full description of the procedures

TABLE 4 Tree attributes by stand type in Lady Park Wood in 2019, including absolute values for trees of all species and all ash trees, relative values for ash and severity of ADB.

Stand type	All trees density (trees ha⁻¹)	Ash tree density (trees ha⁻¹)	Ash tree relative density (% per plot)	All trees basal area (m²ha⁻¹)	Ash basal area (m²ha⁻¹)	Ash relative basal area (% per plot)	All trees dbh (mean cm)	Ash dbh (mean cm)	% ash infected in 2019	Mean ADB severity in 2019 (%)
Old growth	611	92	15%	37.2	8.3	22.4%	20.1	30.3	87%	40%
Young growth	1343	236	18%	28.4	10.6	23.0%	10.9	13.9	85%	47%
Colluvial fan	1258	100	8%	19.1	6.6	34.5%	8.4	22.6	95%	74%
Below cliff	616	70	11%	24.0	7.9	32.7%	14.7	29.3	89%	71%
Managed compartment	1365	190	14%	19.3	6.8	14.3%	16.2	18.7	60%	25%
Mean	1039	138	13%	25.6	8.0	25.4%	14.1	23.0	83%	51%

Abbreviation: ADB, ash dieback.

for selection of beta distribution, variable elimination, model selection and the top models is shown in Supporting Information.

3 | RESULTS

3.1 | Summary statistics

The annual rate of mortality (AMR) of ash trees increased greatly since ADB was first recorded in the woodland in 2013. In the young-growth stands, from an initial population of 376, AMR was 0.1% during 1992–2013 and 1.4% (of 368 trees) during 2013–2019, and in the old-growth stands AMR was 0.4% (of 107 trees) and 1.8% (of 98 trees) in the two periods, respectively. All other stand types also showed a marked increase in AMR since 2013.

Across the woodland, the proportion of all recorded ash trees that were infected with ADB by 2019 was 81% (the mean of the values per stand type was 83%, Table 4). This had increased to 95% by 2020. There was also a marked increase in the proportion of recorded ash trees with >80% crown dieback from 24.5% in 2019 to 41% in 2020. Ash trees that had a below-canopy crown position in 2013 had a markedly higher severity of ADB in 2019 and to a lesser extent in 2020 than those with a canopy or sub-canopy crown position (Figure 3). The proportion of ash trees infected and the severity of ADB were greatest in the stands on the colluvial fan and below the cliff, which are adjacent to a wide river (Figure 1) and have moister soils (Peterken & Mountford, 2017) and where ash accounts for the highest proportion of the total basal area (Table 4). In contrast, both the proportion of infected ash trees and severity of infection were notably lower in the managed compartment (in which ash accounts for the lowest proportion of the total basal area and where there has been recent thinning of trees) than in all the unmanaged compartments (Table 4). However, no consistent associations were found, at the whole stand level, between the incidence of ADB infection and tree density (of all species and of the absolute and relative density of ash specifically).

3.2 | Nonspatial modelling

Results from the model selection procedure are provided in full in Supporting Information. The resulting models for the prediction of ADB in 2019 by the nonspatial predictors outlined in Table 3 included stand type and six other variables that made an independent contribution to the variation between trees in their severity of ADB (Figure 4; Table 5). There is strong evidence that greater ADB severity was associated with smaller 2013 diameter at breast height, lower relative growth rate (between 2000–2002 and 2013) and lower soil pH. The severity of ADB was much less in the young-growth and old-growth stand types than in the below cliff and colluvial fan stand types. It was only very weakly associated with longer-term past relative growth rate, density of ash trees in the same subplot or slope gradient.
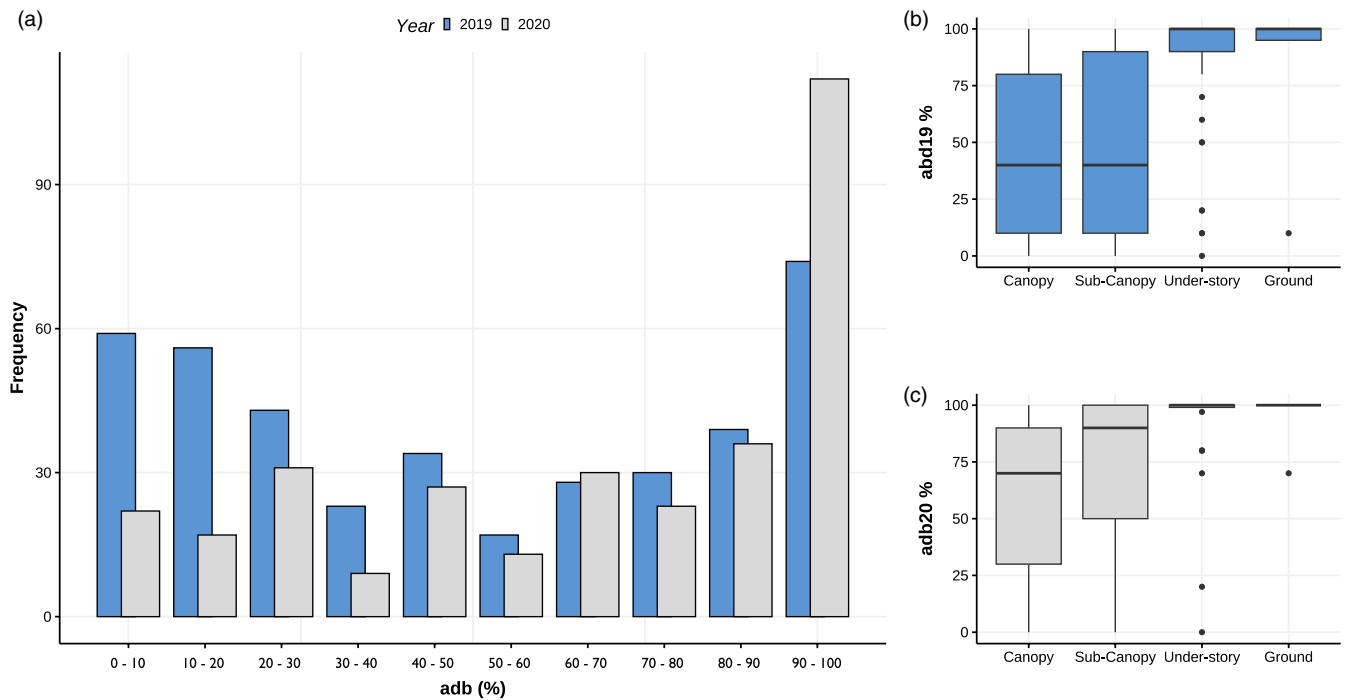
FIGURE 3 Severity of ash dieback (ADB) (level of crown defoliation of ash trees): (a) across the whole woodland in 2019 and 2020 shown as frequency of the number of trees scored in each 10% class of defoliation; (b) box-and-whisker plot of ADB severity in the section of the forest with the greatest density of ash trees, the young-growth stands, for trees with each of four crown positions in 2019 and (c) 2020. Trees with crowns in the canopy and subcanopy are clearly less affected than those in the understorey and near the ground. Dieback severity increased in canopy and subcanopy trees between 2019 and 2020.

3.3 | Spatial modelling

The models resulting from the selection procedure (see Supporting Information) for the prediction of ADB in 2019 by the spatial predictors outlined in Tables 2 and 3 included stand type and four other variables that made an independent contribution to the variation between trees in their severity of ADB (Figure 5; Table 6). Greater ADB severity was strongly associated with greater weighted species mingling (i.e. a lower proportion of conspecific trees amongst the six nearest neighbours of the focal trees weighted by their species richness). The sensitivity analysis showed that use of the basic species mingling index (mi6) in place of the weighted index (wmi6) had a minimal effect on the model results (Tables S4 and S5). Greater ADB severity was also significantly associated with smaller 2013 diameter at breast height (Figure 5; Table 6). The severity of ADB was much less in the young growth, old growth and especially in the managed compartment stand types than in the below cliff and colluvial fan stand types. It was only very weakly associated with local tree density or basal area of larger trees and was not independently associated with size dominance of the focal tree.

4 | DISCUSSION

The level of ADB reached at the early-mid stage of the epidemic in Lady Park Wood was clearly linked to site environment factors. The generalised linear mixed effects models (GLMM) results showed that there was a very large and significant difference in severity of the disease amongst the stand types occupying different topographic positions and with different management histories within the woodland. The high incidence of disease in the colluvial fan and below cliff sites are as expected from previous studies reporting greater infection in sites with moist soils (e.g. Havrdová et al., 2017; Muñoz et al., 2016; Skovsgaard et al., 2017), which is generally attributed to greater production of inoculum from litter and is associated with a greater occurrence of basal lesions (Marçais et al., 2016). Topographic and substrate factors may also influence crown dieback symptoms via their impact on rooting depth and drainage (Skovsgaard et al., 2017). Our observations of variation amongst the topographic zones indicate that trees on the lower slopes and upper steep slopes were much more severely affected than those on the intermediate mid-slopes (which have greater moisture retention during drought), and there is existing evidence of the importance of this moisture variation on tree ecophysiology at Lady Park Wood (Peterken & Mountford, 2017). Cavin et al. (2013) studied the long-term effects of drought events and found that they can lead to changes in the competition dynamics amongst the tree species' populations. Given that ash is known to be susceptible to drought (Berger et al., 2010; Dobrowolska et al., 2011; Drenkhan et al., 2014; Zollner & Kölling, 1994), it is possible that trees on sites subject to greater variation in moisture availability have reduced resistance to ADB. The low incidence and significantly lower severity of ADB in the managed compartment that has been subject to recent thinning is also a striking result.
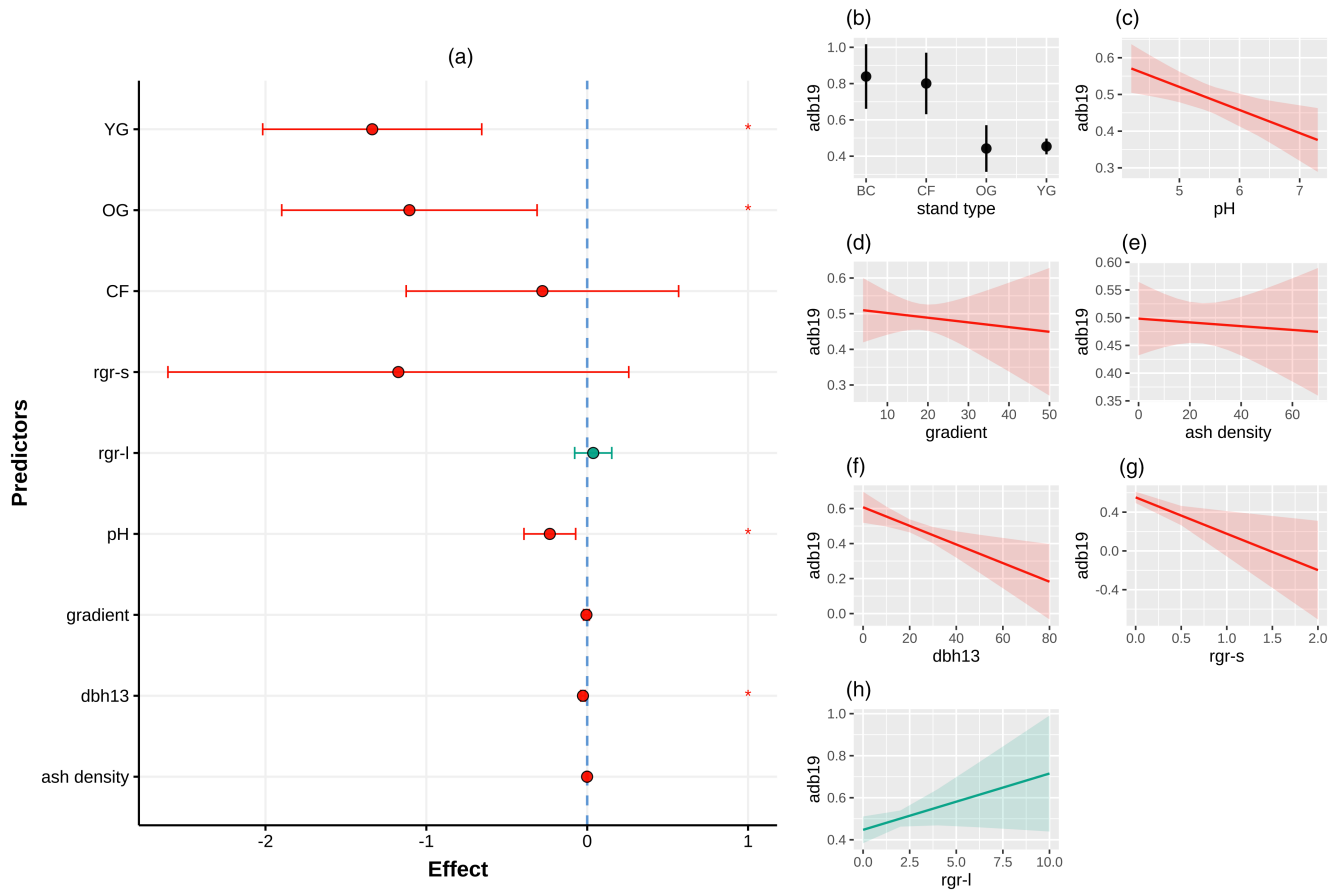
FIGURE 4 Nonspatial model (a) Effect (model average coefficient) of nonspatial predictors on adb19 severity. Single-effect plots of the association of adb19 severity with each retained variable: (b) stand type, (c) pH, (d) gradient, (e) ash density, (f) dbh13, (g) rgr-s and (h) rgr-l. Variable abbreviations are defined in Table 3. All panels include 95% confidence intervals coloured red or green for negative or positive average effects, respectively.

TABLE 5 Nonspatial variables predicting the severity of ash dieback in 2019.

Variable	Estimate	SE	Adjusted SE	z value	Pr(>|z|)	CI lower	CI upper
(intercept)	3.260	0.717	0.720	4.527	<0.01	1.849	4.672
YG	−1.336	0.346	0.347	3.847	<0.01	−2.017	−0.655
OG	−1.105	0.403	0.404	2.729	<0.01	−1.898	−0.311
CF	−0.278	0.430	0.432	0.644	0.519	−1.125	0.568
pH	−0.232	0.081	0.081	2.835	<0.01	−0.393	−0.071
gradient	−0.004	0.009	0.009	0.533	0.593	−0.022	0.012
ash density	−0.0007	0.002	0.002	0.291	0.770	−0.005	0.004
dbh13	−0.026	0.007	0.007	3.736	<0.01	−0.040	−0.012
rgr-s	−1.174	0.729	0.730	1.606	0.108	−2.606	0.258
rgr-l	0.037	0.058	0.058	0.636	0.524	−0.077	0.152

Note: Estimated regression parameters, standard errors (SE), *z*-values, *p*-values and confidence intervals (CI) for model averaging and composite generalised linear mixed effects models of nonspatial variables selected via the procedure outlined in Section 2.4 and models presented in Table S3. Variable abbreviations are defined in Table 3.

Our first question was derived from previous research that found a clear positive association between higher levels of ADB and dense, unthinned stands (Bakys et al., 2013; Skovsgaard et al., 2017), with lower levels amongst dispersed ash trees in an agricultural matrix than within woodland at a landscape scale (Grosdidier et al., 2020). However, the results of the present study showed no marked relationship between incidence or severity of ADB and the density of trees (of all species) at the whole stand level or between severity of
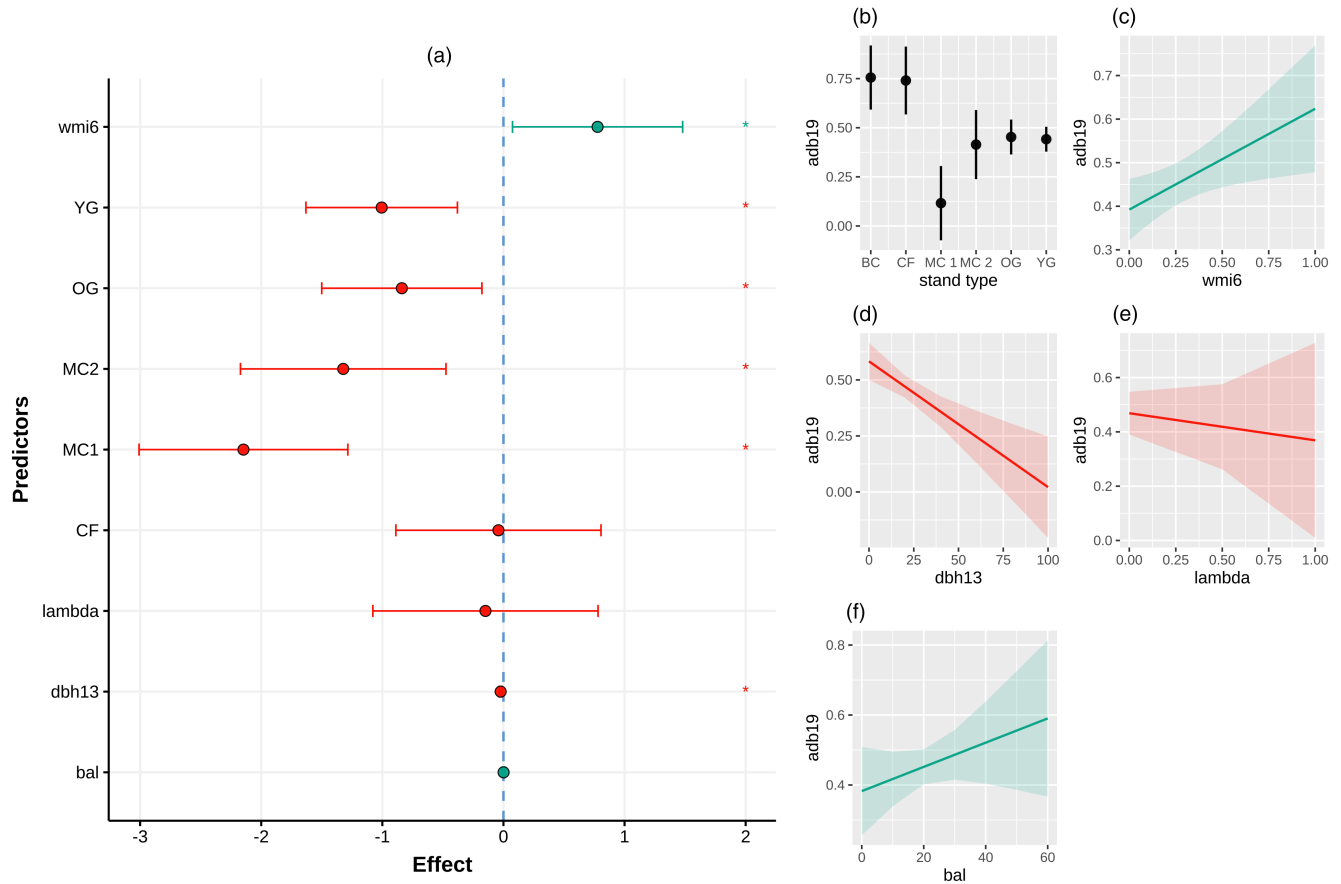
FIGURE 5 Spatial model (a) Effect (model average coefficient) of spatial predictors on adb19 severity. Single-effect plots of the association of adb19 severity with each retained variable: (b) stand type, (c) wmi6, (d) dbh13, (e) lambda and (f) bal. Variable abbreviations are defined in Table 3. All panels include 95% confidence intervals coloured red or green for negative or positive average effects, respectively.

TABLE 6 Spatial variables predicting the severity of ash dieback in 2019.

Variable	Estimate	SE	Adjusted SE	z value	Pr(>|z|)	CI lower	CI upper
(intercept)	1.157	0.386	0.387	2.988	<0.01	0.398	1.916
YG	−1.005	0.318	0.319	3.151	<0.01	−1.631	−0.380
OG	−0.839	0.337	0.337	2.486	0.012	−1.500	−0.178
CF	−0.041	0.431	0.432	0.096	0.923	−0.888	0.806
MC1	−2.147	0.439	0.440	4.881	<0.01	−3.009	−1.285
MC2	−1.323	0.432	0.433	3.056	<0.01	−2.172	−0.474
wmi6	0.777	0.357	0.358	2.169	0.030	0.075	1.480
dbh13	−0.023	0.006	0.006	3.830	<0.01	−0.035	−0.011
lambda	−0.148	0.473	0.474	0.313	0.754	−1.078	0.781
bal	0.001	0.005	0.005	0.220	0.826	−0.009	0.011

Note: Estimated regression parameters, standard errors (SE), z-values, p-values and confidence intervals (CI) for model averaging and composite generalised linear mixed effects models of spatial variables selected via the procedure outlined in Section 2.4 and models presented in Table S4. Variable abbreviations are defined in Table 3.

ADB and local tree density around individual focal ash trees calculated using a kernel function (lambda); hence, our answer to the first question is 'no'.

Site and neighbourhood effects could occur through either their influence on the rate of transmission of ascospores or on the resistance to infection of ash trees mediated by their physiological condition. It is unlikely that, at this stage of the epidemic, spatial variation (at stand and individual tree scales) in the density of *H. fraxineus* ascospores is the primary cause of the variation in ADB severity of individual trees recorded in the present study within

an unfragmented closed-canopy woodland. This finding is strongly supported by the GLMM result showing a lack of any meaningful relationship between severity of ADB and the density of ash trees in the same subplot as the focal tree. In 2019, 2 years after ADB was first recorded in this well-monitored site, overall, 81% of ash trees were infected, and that had increased markedly to 95% by the following summer of 2020. It is likely, therefore, that the density of dispersed ascospores across the site was already so high that every susceptible ash tree was subject to a high inoculum load. ADB of a single tree produces millions of tiny ascospores that disperse widely even in dry conditions (estimated mean dispersal distance 0.2–2.6 km (Grosdidier et al., 2018)), though with a rapid decline in dispersed inoculum density up to 50 m from an infected host (Chandelier et al., 2014). In this context, the large differences in both infection rate and, to an even greater extent, severity observed amongst the different stands in the study woodland at this early-mid stage of the epidemic are notable, and the stands with the highest percentage of trees infected and severity of ADB had only moderate or low absolute density and basal area of ash trees (Table 4).

Our second question addressed the alternative mechanism explaining variation between ash trees in their severity of ADB: that their resistance to or recovery from infection is mediated by their physiological condition, for example, earlywood vessel size and slower growth feeding back and amplifying crown dieback (Klesse et al., 2020; Skovsgaard et al., 2017). To assess this, it is a unique strength of the present study that Lady Park Wood has a long record of the prior growth rates of individual ash trees in permanent sample plots as a valuable indicator of their condition. This revealed a strong negative association between severity of ADB and relative stem radial growth rates during the 11 years immediately prior to the first observation of the disease in the woodland. This provides robust evidence to answer yes to the second question: trees in a more vigorous condition had greater resistance to the disease. This result is compatible with earlier studies based on less precise evidence that showed a negative relationship between the severity of ADB and tree 'vitality' in Scandinavia (Bengtsson et al., 2021; Timmermann et al., 2017), and the conclusion of Skovsgaard et al. (2017) that vigorous trees can better compensate for the effects of *H. fraxineus*. Previous studies have also shown that tree height can be a significantly strong predictor of lower rates of ADB defoliation (Erfmeier et al., 2019), as well as individual tree vigour (Dobbertin, 2005), and our result that lower ADB severity is significantly associated with a larger diameter at breast height matches the findings of previous studies (e.g. Enderle et al., 2019; Klesse et al., 2021; Marçais et al., 2016; Skovsgaard et al., 2010). It may be that such a negative association between recorded severity of ADB and tree size at the earlier stages of an epidemic may simply be a matter of time, with the infection taking longer to penetrate all the vascular tissue of larger diameter individuals (Erfmeier et al., 2019; Thomas, 2016). Other studies have suggested that in time ADB can infect ash trees of all sizes and ages (Pautasso et al., 2013).

Tree growth rates integrate many factors, including genotype, site environment and (as the basis for our third question) influence exerted by nearest neighbour trees, which may have differential impacts on resistance to ADB. The evidence for the effect of site environment factors was reviewed above. Our results provide only limited evidence that the lower the level of neighbour competition on an ash tree, the lower its severity of ADB at this stage of the epidemic. We found a quantitative indication (Figure 3) that taller ash trees with crowns scored as having canopy and subcanopy crown positions had much lower severity of ADB than those with crowns below the canopy; however, this was not corroborated by the spatial GLMM model result showing no association of ADB severity with the basal area of larger trees. Therefore, our results only provide equivocal evidence for an answer of yes to the third question.

A striking result of the spatial GLMM was that the severity of ADB was significantly positively associated with a lower proportion of conspecific ash trees amongst the six nearest neighbour trees of a focal ash tree weighted by their species richness (as shown by the weighted species mingling index and corroborated by both the strong correlation of this index with the basic species mingling index and the equivalence of the model results obtained with the basic index in the sensitivity analysis). The direction of this result was contrary to the expectation of the fourth question. Grossman et al. (2019), in a temperate forest, and Rutten et al. (2021) in a subtropical forest, also reported the occurrence of both positive and negative effects of a more species-diverse tree neighbourhood on the susceptibility to disease of individual tree species. Keesing et al. (2006) described a suite of mechanisms whereby species richness can either decrease or increase disease risk including the 'dilution effect' where increased density of heterospecific neighbours reduces infection rates (Mitchell et al., 2002). Some other reported mechanisms can be excluded in the context of the present study as *H. fraxineus* is not known to have alternative host species amongst the flora of Lady Park Wood and animal vectors are not thought to be important in its transmission. Previous studies have indicated a distance component of other species mixture effects. Murrell and Law (2003) postulated that interspecies competition occurs at shorter distances than intraspecies competition ('heteromyopia') and a reversal of tree interaction effects between shorter and longer distances has been demonstrated in various other contexts (Pommerening & Sánchez Meador, 2018). The evidence available from the present study does not allow the contradiction amongst these findings to be resolved and this stands out as a priority for future research. This will be important to provide a stronger mechanistic basis for the widely held view that mixed-species stands, as opposed to monocultures, have a reduced susceptibility to tree diseases (Pautasso et al., 2005), which has been supported by the results of a recent systematic review (Roberts et al., 2020).

There is evidence that the species identity of the near neighbours of ash trees can influence, either positively or negatively,

the severity of their ADB specifically (Havrdová et al., 2017). Therefore, key to understanding the mechanisms of the species mingling result will be an analysis of the difference in the effect of individual species of neighbouring tree present at Lady Park Wood. Some inference can be drawn from existing knowledge of the key species. In terms of above-ground competition from the abundant canopy species, it is *F. sylvatica* and *Tilia* spp. that cast the densest shade (Ellenberg, 1988). The level of below-ground competition from different neighbouring species is likely to interact with site substrate properties. *Fagus sylvatica*, an abundant species in many areas of Lady Park Wood, is also highly competitive for below-ground resources, especially in certain soil layers (Bolte et al., 2013; Pretzsch et al., 2010). It is water demanding; however, as a result its importance as a competitor may have been diminished due to its elevated mortality rate and the long-term reduction in its growth rates following the drought of 1976 (Cavin et al., 2013). The role of *F. sylvatica* trees as competitive neighbours is known to be complex: in old-growth forests, high levels of conspecific above-ground competition (shading) on *F. sylvatica* trees were found to reduce or even reverse the negative effects of below-ground competition (Fichtner et al., 2015).

Instead of being a result of competition, neighbouring tree effects could be mediated by the influence of their leaf litter chemistry. For example, Havrdová et al. (2017) found that ADB severity was greater in ash trees where *F. sylvatica*, *Quercus* spp. and *Betula pendula* were present in their neighbourhood and lower in the presence of *Abies* spp., *Pinus* spp. and *Acer* spp. They suggest that this could be explained by the interaction of different chemical and physical characteristics of the litter of different species, leading to different rates of leaf decomposition in species mixtures and a consequent effect on the degradation of ash petioles and thus ADB ascospore production.

It is therefore a priority for future research to test the relationship between severity of ADB and the species identity, as well as relative size, of neighbouring trees. Such evidence would indicate the value of making greater use of NNSS based on species identity. Relative size of nearest neighbours is, however, likely to remain the dominant factor via its effect on the vigour of the focal tree (Pommerening & Sánchez Meador, 2018). Species identity is thus likely to be most important for dominant 'monumental' individuals in influencing the composition and spatial structure of trees in their neighbourhood (Cholewińska et al., 2021).

The unique dataset provided by the permanent sample plots at Lady Park Wood has enabled a statistical modelling procedure that provides evidence of at least four significant effects on the severity of ADB of individual ash trees at this early-mid stage of the epidemic. The procedure narrowed the selection of potential predictor variables and indicates the potential for the untested factor of genotypic variation in resistance amongst individual ash trees (not linked to their prior growth rate) to account for a high proportion of variation in their severity of infection, as well as the inherently stochastic nature of the infection process. While this

supports findings that there may be sufficient genetic variation within the ash population on which natural selection for greater disease resistance may act (Stener, 2018; Stocks et al., 2019), the notable increase in percentage of infected trees between the sixth and seventh years after first detection of the pathogen in Lady Park Wood (from 81% to 95%) reduces this optimism. Future monitoring will be crucial to determine what proportion of the ash trees have sufficient resistance to survive the infection and subsequently set seed.

The findings of our research have advanced those of previous studies (e.g. Grosdidier et al., 2020) by highlighting the influence of individual tree neighbourhood effects within mixed-species forests, as well as reinforcing at an intensive population scale the findings of Klesse et al. (2021) concerning a tree's previous relative growth rate as a separate effect from its size. They do not support growing ash in tree species mixtures as an effective measure to reduce the severity of ADB. However, they do indicate the potential contribution of silvicultural measures aimed at establishing species mingling patterns, and thinning targeted at reducing competition levels, based on the species of neighbouring trees as well as their relative size, in addition to genetic selection, all targeted at increasing the vigour of ash trees in order to increase their resistance to subsequent ADB infection.

AUTHOR CONTRIBUTIONS

George Peterken recorded the ash population in 2013–2015 in anticipation of ADB and was responsible with many others for accumulating the earlier records. David Cracknell and George Peterken designed the study with John Healey. David Cracknell collected most of the 2019/2020 data. David Cracknell processed and analysed the historic data and maps, did all the initial data analysis and led the writing of the manuscript. John Healey advised on data analysis and contributed to writing the manuscript. Arne Pommerening advised on the selection and use of point process statistics, wrote the corresponding R code and contributed to the methods section and analysis. Peter Lawrence carried out the statistical procedure and GLMM modelling and redrafted corresponding parts of the manuscript. All authors contributed critically and edited the manuscript and gave final approval for publication.

CONFLICT OF INTEREST STATEMENT

The authors declare that there are no conflicts of interest.

PEER REVIEW

The peer review history for this article is available at https://www.webofscience.com/api/gateway/wos/peer-review/10.1111/1365-2745.14191.

DATA AVAILABILITY STATEMENT

Supplementary material and datasets are available at Dryad Digital Repository https://doi.org/10.5061/dryad.ngf1vhhxg (Cracknell et al., 2023).

ORCID

David J. Cracknell https://orcid.org/0000-0002-2428-2335
George F. Peterken https://orcid.org/0000-0003-2187-1457
Arne Pommerening https://orcid.org/0000-0002-3441-2391
Peter J. Lawrence https://orcid.org/0000-0002-9809-0221
John R. Healey https://orcid.org/0000-0002-5398-2293

REFERENCES

Aguirre, O., Hui, G., Gadow, K., & Jimenez, J. (2003). An analysis of spatial forest structure using neighbourhood-based variables. *Forest Ecology and Management*, *183*, 137–145.

Baddeley, A., Rubak, E., & Turner, R. (2015). *Spatial point patterns: Methodology and applications with R*. Taylor & Francis Group. https://doi.org/10.1201/b19708

Bakys, R., Vasaitis, R., & Skovsgaard, J. P. (2013). Patterns and severity of crown dieback in young even-aged stands of European ash (*Fraxinus excelsior* L.) in relation to stand density, bud flushing phenotype, and season. *Plant Protection Science*, *49*, 120–126. https://doi.org/10.17221/70/2012-pps

Bartoń, K. (2022). *MuMIn: Multi-model inference (1.46.0)*. https://CRAN.R-project.org/package=MuMIn

Bengtsson, V., Stenström, A., Wheater, C. P., & Sandberg, K. (2021). The impact of ash dieback on veteran trees in southwestern Sweden. *Baltic Forestry*, *27*, 558. https://doi.org/10.46490/BF558

Berger, R., Heydeck, P., Baumgart, A., & Roloff, A. (2010). Neue ergebnisse zum eschentriebsterben. *AFZ-Wald*, *65*, 18–21.

Bolte, A., Kampf, F., & Hilbrig, L. (2013). Space sequestration below ground in old-growth spruce-beech forests-signs for facilitation? *Frontiers in Plant Science*, *4*, 322. https://doi.org/10.3389/fpls.2013.00322

Bowler, A. (2019). *Trends in research surrounding Chalara ash dieback (Hymenoscyphus fraxineus) between 1992 and 2019—A systematic review* (MSc dissertation). Bangor University.

British Ecological Society. (2012). *First occurrence of 'ash dieback' in Britain*. Ecology and Policy Blog. http://www.britishecologicalsociety.org/first-occurrence-of-ash-dieback-in-britain/

Burnham, K. P., Anderson, D. R., & Huyvaert, K. P. (2011). AIC model selection and multimodel inference in behavioral ecology: Some background, observations, and comparisons. *Behavioral Ecology and Sociobiology*, *65*, 23–35.

Cavin, L., Mountford, E. P., Peterken, G. F., & Jump, A. S. (2013). Extreme drought alters competitive dominance within and between tree species in a mixed forest stand. *Functional Ecology*, *27*, 1424–1435. https://doi.org/10.1111/1365-2435.12126

Chandelier, A., Helson, M., Dvorak, M., & Gischer, F. (2014). Detection and quantification of airborne inoculum of *Hymenoscyphus pseudoalbidus* using real-time PCR assays. *Plant Pathology*, *63*, 1296–1305.

Cholewińska, O., Keczyński, A., Kusińska, B., & Jaroszewicz, B. (2021). Species identity of large trees affects the composition and the spatial structure of adjacent trees. *Forests*, *12*, 1162. https://doi.org/10.3390/f12091162

Chumanová, E., Romportl, D., Havrdová, L., Zahradník, D., Pešková, V., & Černý, K. (2019). Predicting ash dieback severity and environmental suitability for the disease in forest stands. *Scandinavian Journal of Forest Research*, *34*, 254–266. https://doi.org/10.1080/02827581.2019.1584638

Coker, T. L. R., Rozsypálek, J., Edwards, A., Harwood, T. P., Butfoy, L., & Buggs, R. J. (2019). Estimating mortality rates of European ash (*Fraxinus excelsior*) under the ash dieback (*Hymenoscyphus fraxineus*) epidemic. *Plants, People, Planet*, *1*, 48–58. https://doi.org/10.1002/ppp3.11

Cracknell, D. J., Peterken, G. F., Pommerening, A., Lawrence, P. J., & Healey, J. R. (2023). Data Neighbours matter and the weak succumb: Ash dieback infection is more severe in ash trees with fewer conspecific neighbours and lower prior growth rate. *Dryad Digital Repository*, https://doi.org/10.5061/dryad.ngf1vhhxg

Delignette-Muller, M. L., Dutang, C., Pouillot, R., Denis, J. B., & Siberchicot, A. (2015). Package 'fitdistrplus'. *Journal of Statistical Software*, *64*, 1–34.

Diggle, P. J. (1985). A kernel method for smoothing point process data. *Journal of the Royal Statistical Society: Series C: Applied Statistics*, *34*, 138–147.

Dobbertin, M. (2005). Tree growth as indicator of tree vitality and of tree reaction to environmental stress: A review. *European Journal of Forest Research*, *124*, 319–333. https://doi.org/10.1007/s10342-005-0085-3

Dobrowolska, D., Hein, S., Oosterbaan, A., Wagner, S., Clark, J., & Skovsgaard, J. P. (2011). A review of European ash (*Fraxinus excelsior* L.): Implications for silviculture. *Forestry*, *84*, 133–148. https://doi.org/10.1093/forestry/cpr001

Dormann, C. F., Calabrese, J. M., Guillera-Arroita, G., Matechou, E., Bahn, V., Bartoń, K., Beale, C. M., Ciuti, S., Elith, J., Gerstner, K., Guelat, J., Keil, P., Lahoz-Monfort, J. J., Pollock, L. J., Reineking, B., Roberts, D. R., Schröder, B., Thuiller, W., Warton, D. I., … Hartig, F. (2018). Model averaging in ecology: A review of Bayesian, information-theoretic, and tactical approaches for predictive inference. *Ecological Monographs*, *88*, 485–504. https://doi.org/10.1002/ecm.1309

Drenkhan, R., Sander, H., & Hanso, M. (2014). Introduction of Mandshurian ash (*Fraxinus mandshurica* Rupr.) to Estonia: Is it related to the current epidemic on European ash (*F. excelsior* L.)? *European Journal of Forest Research*, *133*, 769–781.

Ellenberg, H. (1988). *Vegetation ecology of Central Europe*. Cambridge University Press.

Enderle, R., Metzler, B., Riemer, U., & Kändler, G. (2018). Ash dieback on sample points of the national forest inventory in South-Western Germany. *Forests*, *9*, 25. https://doi.org/10.3390/f9010025

Enderle, R., Stenlid, J., & Vasaitis, R. (2019). An overview of ash (*Fraxinus* spp.) and the ash dieback disease in Europe. *CAB Reviews*, *14*, 025. https://doi.org/10.1079/PAVSNNR201914025

Erfmeier, A., Haldan, K. L., Beckmann, L. M., Behrens, M., Rotert, J., & Schrautzer, J. (2019). Ash dieback and its impact in near-natural forest remnants—A plant community-based inventory. *Frontiers in Plant Science*, *10*, 658. https://doi.org/10.3389/fpls.2019.00658

Fichtner, A., Forrester, D. I., Härdtle, W., Sturm, K., & Von Oheimb, G. (2015). Facilitative-competitive interactions in an old-growth forest: The importance of large-diameter trees as benefactors and stimulators for forest community assembly. *PLoS ONE*, *10*, e0120335. https://doi.org/10.1371/journal.pone.0120335

Gadow, K. V. (1993). Zur Bestandesbeschreibung in der Forsteinrichtung [New variables for describing stands of trees]. *Forst und Holz*, *48*, 602–606.

Gadow, K. V., González, J. G. Á., Zhang, C., Pukkala, T., & Zhao, X. (2021). *Sustaining forest ecosystems*. Springer Nature.

Grosdidier, M., Ioos, R., Husson, C., Cael, O., Scordia, T., & Marçais, B. (2018). Tracking the invasion: Dispersal of *Hymenoscyphus fraxineus* airborne inoculum at different scales. *FEMS Microbiology Ecology*, *94*, fiy049. https://doi.org/10.1093/femsec/fiy049

Grosdidier, M., Scordia, T., Ioos, R., & Marçais, B. (2020). Landscape epidemiology of ash dieback. *Journal of Ecology*, *108*, 1789–1799. https://doi.org/10.1111/1365-2745.13383

Gross, A., Holdenrieder, O., Pautasso, M., Queloz, V., & Sieber, T. N. (2014). *Hymenoscyphus pseudoalbidus*, the causal agent of European ash dieback. *Molecular Plant Pathology*, *15*, 5–21. https://doi.org/10.1111/mpp.12073

Grossman, J. J., Cavender-Bares, J., Reich, P. B., Montgomery, R. A., & Hobbie, S. E. (2019). Neighbourhood diversity simultaneously increased and decreased susceptibility to contrasting herbivores in an early-stage forest diversity experiment. *Journal of Ecology*, *107*, 1492–1505. https://doi.org/10.1111/1365-2745.13097

Hanisch, K. H. (1984). Some remarks on estimators of the distribution function of nearest neighbour distance in stationary spatial point processes. *Mathematische Operationsforschung und Statistik, Series Statistics*, *15*, 409–412. https://doi.org/10.1080/02331888408801788

Havrdová, L., Novotná, K., Zahradník, D., Buriánek, V., Pešková, V., Šrůtka, P., & Černý, K. (2016). Differences in susceptibility to ash dieback in Czech provenances of *Fraxinus excelsior*. *Forest Pathology*, *46*, 281–288. https://doi.org/10.1111/efp.12265

Havrdová, L., Zahradník, D., Romportl, D., Pešková, V., & Černý, K. (2017). Environmental and silvicultural characteristics influencing the extent of ash dieback in forest stands. *Baltic Forestry*, *23*, 168–182.

Hui, G., Zhao, X., Zhao, Z., & von Gadow, K. (2011). Evaluating tree species spatial diversity based on neighborhood relationships. *Forest Science*, *57*, 292–300. https://doi.org/10.1093/forestscience/57.4.292

Hui, Y., Albert, M., & Gadow, K. (1998). Diameter dominance as a parameter for simulating forest structure. *Forstwissenschaftliches Centralblatt*, *117*, 258–266.

Illian, J., Penttinen, A., Stoyan, H., & Stoyan, D. (2008). *Statistical analysis and modelling of spatial point patterns*. John Wiley & Sons. https://doi.org/10.1002/9780470725160

Keesing, F., Holt, R. D., & Ostfeld, R. S. (2006). Effects of species diversity on disease risk. *Ecology Letters*, *9*, 485–498. https://doi.org/10.1111/j.1461-0248.2006.00885.x

Kjær, E. D., McKinney, L. V., Nielsen, L. R., Hansen, L. N., & Hansen, J. K. (2012). Adaptive potential of ash (*Fraxinus excelsior*) populations against the novel emerging pathogen *Hymenoscyphus pseudoalbidus*. *Evolutionary Applications*, *5*, 219–228. https://doi.org/10.1111/j.1752-4571.2011.00222.x

Klesse, S., Abegg, M., Hopf, S. E., Gossner, M. M., Rigling, A., & Queloz, V. (2021). Spread and severity of ash dieback in Switzerland—Tree characteristics and landscape features explain varying mortality probability. *Frontiers in Forests and Global Change*, *4*, Article 645920. https://doi.org/10.3389/ffgc.2021.645920

Klesse, S., von Arx, G., Gossner, M. M., Hug, C., Rigling, A., & Queloz, V. (2020). Amplifying feedback loop between growth and wood anatomical characteristics of *Fraxinus excelsior* explains size-related susceptibility to ash dieback. *Tree Physiology*, *41*, 683–696. https://doi.org/10.1093/treephys/tpaa091

Kowalski, T. (2006). *Chalara fraxinea* sp. nov. associated with dieback of ash (*Fraxinus excelsior*) in Poland. *Forest Pathology*, *36*, 264–270. https://doi.org/10.1111/j.1439-0329.2006.00453.x

Lenz, H. D., Bartha, B., Straßer, L., & Lemme, H. (2016). Development of ash dieback in South-Eastern Germany and increasing occurrence of secondary pathogens. *Forests*, *7*, 41. https://doi.org/10.3390/f7020041

Lenz, H. D., Straßer, L., Baumann, M., & Baier, U. (2012). Boniturschlüssel zur Einstufung der Vitalität von Alteschen. *AFZ-DerWald*, *67*(3), 18–19.

Marçais, B., Husson, C., Caël, O., Saintonge, F.-X., Delahaye, L., Collet, C., & Chandelier, A. (2017). Estimation of ash mortality induced by Hymenoscyphus fraxineus in France and Belgium. *Baltic Forestry*, *23*, 159–167.

Marçais, B., Husson, C., Godart, L., & Caël, O. (2016). Influence of site and stand factors on *Hymenoscyphus fraxineus*-induced basal lesions. *Plant Pathology*, *65*, 1452–1461. https://doi.org/10.1111/ppa.12542

Mazerolle, M. J., & Mazerolle, M. M. J. (2017). *Package 'AICcmodavg'*. R package, 281.

McKinney, L. V., Nielsen, L. R., Collinge, D. B., Thomsen, I. M., Hansen, J. K., & Kjær, E. D. (2014). The ash dieback crisis: Genetic variation in resistance can prove a long-term solution. *Plant Pathology*, *63*, 485–499. https://doi.org/10.1111/ppa.12196

Mitchell, C. E., Tilman, D., & Groth, J. V. (2002). Effects of grassland plant species diversity, abundance, and composition on foliar fungal disease. *Ecology*, *83*, 1713–1726. https://doi.org/10.1890/0012-9658(2002)083[1713:EOGPSD]2.0.CO;2

Mitchell, R., Bailey, S., Beaton, J. K., Bellamy, P. E., Brooker, R. W., Broome, A., Chetcuti, J., Eaton, S., Ellis, C. J., Farren, J., Gimona, A., Goldberg, E., Hall, J., Harmer, R., Hester, A. J., Hewison, R. L., Hodgetts, N. G., Hooper, R. J., Howe, L., ... Woodward, S. (2014). *The potential ecological impact of ash dieback in the UK*. JNCC Report No. 483. https://hub.jncc.gov.uk/assets/1352bab5-3914-4a42-bb8a-a0a1e2b15f14

Muñoz, F., Marçais, B., Dufour, J., & Dowkiw, A. (2016). Rising out of the ashes: Additive genetic variation for crown and collar resistance to *Hymenoscyphus fraxineus* in *Fraxinus excelsior*. *Phytopathology*, *106*, 1535–1543.

Murrell, D. J., & Law, R. (2003). Heteromyopia and the spatial coexistence of similar competitors. *Ecology Letters*, *6*, 48–59. https://doi.org/10.1046/j.1461-0248.2003.00397.x

Nemesio-Gorriz, M., McGuinness, B., Grant, J., Dowd, L., & Douglas, G. C. (2019). Lenticel infection in *Fraxinus excelsior* shoots in the context of ash dieback. *iForest*, *12*, 160–165. https://doi.org/10.3832/ifor2897-012

Pautasso, M., Aas, G., Queloz, V., & Holdenrieder, O. (2013). European ash (*Fraxinus excelsior*) dieback—A conservation biology challenge. *Biological Conservation*, *158*, 37–49. https://doi.org/10.1016/j.biocon.2012.08.026

Pautasso, M., Holdenrieder, O., & Stenlid, J. (2005). Susceptibility to fungal pathogens of forests differing in tree diversity. *Forest Diversity and Function*, *176*, 263–289. https://doi.org/10.1007/3-540-26599-6_13

Peterken, G., & Mountford, E. (2017). *Woodland development: A long-term study of Lady Park Wood*. CABI International.

Pommerening, A., & Grabarnik, P. (2019). *Individual-based methods in forest ecology and management*. Springer. https://doi.org/10.1007/978-3-030-24528-3

Pommerening, A., & Sánchez Meador, A. J. (2018). Tamm review: Tree interactions between myth and reality. *Forest Ecology and Management*, *424*, 164–176. https://doi.org/10.1016/j.foreco.2018.04.051

Pretzsch, H., Block, J., Dieler, J., Dong, P. H., Kohnle, U., Nagel, J., Spellman, H., & Zingg, A. (2010). Comparison between the productivity of pure and mixed stands of Norway spruce and European beech along an ecological gradient. *Annals of Forest Science*, *67*, 712.

Queloz, V. (2016). Eschentriebsterben. Sterben ausgewachsene Eschen auch ab? *Wald und Holz*, *97*(6), 23–26.

R Core Team. (2021). *R: A language and environment for statistical computing*. R Foundation for Statistical Computing.

Roberts, M., Gilligan, C. A., Kleczkowski, A., Hanley, N., Whalley, A. E., & Healey, J. R. (2020). The effect of forest management options on forest resilience to pathogens. *Frontiers in Forests and Global Change*, *3*, 7. https://doi.org/10.3389/ffgc.2020.00007

Rutten, G., Hönig, L., Schwaß, R., Braun, U., Saadani, M., Schuldt, A., Michalski, S. G., & Bruelheide, H. (2021). More diverse tree communities promote foliar fungal pathogen diversity, but decrease infestation rates per tree species, in a subtropical biodiversity experiment. *Journal of Ecology*, *109*, 2068–2080. https://doi.org/10.1111/1365-2745.13620

Sheil, D., Burslem, D. F. R. P., & Alder, D. (1995). The interpretation and misinterpretation of mortality rate measures. *Journal of Ecology*, *83*, 331–333. https://doi.org/10.2307/2261571

Skovsgaard, J. P., Thomsen, I. M., Skovsgaard, I. M., & Martinussen, T. (2010). Associations among symptoms of dieback in even-aged stands of ash (*Fraxinus excelsior* L.). *Forest Pathology*, *40*, 7–18.

Skovsgaard, J. P., Wilhelm, G. J., Thomsen, I. M., Metzler, B., Kirisits, T., Havrdová, L., Enderle, R., Dobrowolska, D., Cleary, M., & Clark, J. (2017). Silvicultural strategies for *Fraxinus excelsior* in response to dieback caused by *Hymenoscyphus fraxineus*. *Forestry*, *90*, 455–472. https://doi.org/10.1093/forestry/cpx012

Stener, L.-G. (2018). Genetic evaluation of damage caused by ash dieback with emphasis on selection stability over time. *Forest Ecology and Management*, *409*, 584–592. https://doi.org/10.1016/j.foreco.2017.11.049

Stocks, J. J., Buggs, R. J. A., & Lee, S. J. (2017). A first assessment of *Fraxinus excelsior* (common ash) susceptibility to *Hymenoscyphus fraxineus* (ash dieback) throughout the British Isles. *Scientific Reports*, *7*, 16546. https://doi.org/10.1038/s41598-017-16706-6

Stocks, J. J., Metheringham, C. L., Plumb, W. J., Lee, S. J., Kelly, L. J., Nichols, R. A., & Buggs, R. J. (2019). Genomic basis of European ash tree resistance to ash dieback fungus. *Nature Ecology & Evolution*, *3*, 1686–1696. https://doi.org/10.1038/s41559-019-1036-6

Thomas, P. A. (2016). Biological flora of the British Isles: *Fraxinus excelsior*. *Journal of Ecology*, *104*, 1158–1209. https://doi.org/10.1111/1365-2745.12566

Timmermann, V., Børja, I., Hietala, A. M., Kirisits, T., & Solheim, H. (2011). Ash dieback: Pathogen spread and diurnal patterns of ascospore dispersal, with special emphasis on Norway. *EPPO Bulletin*, *41*, 14–20. https://doi.org/10.1111/j.1365-2338.2010.02429.x

Timmermann, V., Nagy, N. E., Hietala, A. M., Børja, I., & Solheim, H. (2017). Progression of ash dieback in Norway related to tree age, disease history and regional aspects. *Baltic Forestry*, *23*, 150–158.

Turczanski, K., Rutkowski, P., Dyderski, M. K., Wronska-Pilarek, D., & Nowinski, M. (2020). Soil pH and organic matter content affects European ash (*Fraxinus excelsior* L.) crown defoliation and its impact on understory vegetation. *Forests*, *11*, 22. https://doi.org/10.3390/F11010022

Wagenmakers, E. J., & Farrell, S. (2004). AIC model selection using Akaike weights. *Psychonomic Bulletin & Review*, *11*, 192–196.

Wang, H., Zhang, X., Hu, Y., & Pommerening, A. (2021). Spatial patterns of correlation between conspecific species and size diversity in forest ecosystems. *Ecological Modelling*, *457*, 109678. https://doi.org/10.1016/j.ecolmodel.2021.109678

Wang, W., Chen, X., Zeng, W., Wang, J., & Meng, J. (2019). Development of a mixed-effects individual-tree basal area increment model for oaks (*Quercus* spp.) considering forest structural diversity. *Forests*, *10*, 474. https://doi.org/10.3390/f10060474

Wykoff, W. (1990). A basal area increment model for individual conifers in the northern Rocky Mountains. *Forest Science*, *26*, 1077–1104.

Zollner, A., & Kölling, C. (1994). Eschenkulturen auf ungeeigneten Standorten. *Allgemeine Forstzeitung*, *2*, 61–64.

Zuur, A. F., Ieno, E. N., Walker, N., Saveliev, A. A., & Smith, G. (2009). *Mixed effects models and extensions in ecology with R*. Springer. https://doi.org/10.1007/978-0-387-87458-6

SUPPORTING INFORMATION

Additional supporting information can be found online in the Supporting Information section at the end of this article.

Table S1: Chronology of survey activity linked to the variables used in this study. Letters indicated researchers active and collecting data at Lady Park Wood within each period.

Table S2: Comparison of AICc values for three models, including three nearest-tree neighbourhoods of *ui* and *wmi*, and comparing *dbh13* with *ba*. Each model was compared pairwise with its correlated partner.

Table S3: Resulting 'top models' for the non-spatial predictor variables included after checking of collinearity and the maintenance of the researcher questions. Abbreviations are defined in Table 3; *stype* = stand type.

Table S4: Resulting 'top models' for the spatial variables based on the collinear variable removal and the maintenance of the researcher questions. Abbreviations are defined in Table 3; *stype* = stand type

Table S5: Resulting 'top models' for the sensitivity analysis of the spatial variables replacing the variable wmi6 with mi6 based on the collinear variable removal and the maintenance of the researcher questions. Abbreviations are defined in Table 3; *stype* = stand type.

Figure S1: Cullen and Frey plot of the response variable (adb19). The plot depicts in 2-D space the skewness and kurtosis of adb19. The proximity of the blue circular symbol "observation" to the other symbols and shaded area facilitates the selection of the most likely and appropriate distribution for the modelling approach. The analysis was conducted using the 'fitdistrplus' package (Delignette-Muller et al., 2015) and identified the beta distribution as most suitable.

Figure S2: Strength of significant correlations amongst pairs of explanatory non-spatial variables. Red indicates a negative correlation and blue a positive correlation. Abbreviations are defined in Tables 1 and 3; stype = stand type (the managed compartment could not be included as a stand-type predictor variable in the non-spatial modelling because log relative growth rate—short time period (rgr.s) data are not available due to lack of site access to that compartment during 2000-2002 for tree dbh measurement).

Figure S3: Strength of significant correlations amongst pairs of explanatory spatial variables. Red indicates a negative correlation and blue a positive correlation. Abbreviations are defined in Tables 1 and 3; stype = stand type (all five stand types were included in the spatial modelling, with the managed compartment split into two sub-compartments).